

INTERACTION OF AN INTERNAL GRAVITY CURRENT WITH A SUBMERGED CIRCULAR CYLINDER

E. V. Ermanyuk and N. V. Gavrilov

UDC 532.59

The problem of hydrodynamic loads due to the interaction of a gravity current propagating over a bottom channel with a submerged circular cylinder is studied experimentally. It was shown that in the examined range of parameters, the hydrodynamic loads are simulated after Froude. The hydrodynamic loads are maximal if the cylinder lies on the bottom, and they decrease rapidly with increase in the distance from the cylinder to the channel bottom. The effects of mixing and entrainment on the nature of the hydrodynamic loads are considered.

Key words: stratified fluid, gravity current, hydrodynamic load.

Introduction. Gravity currents of various types occur widely in nature. Among them are avalanches, pyroclastic currents resulting from concern volcanic eruptions, mudflows, turbidity currents in oceans, atmospheric phenomena accompanying cold air intrusions, etc. In addition, gravity currents arise from various man-made disasters, for example, the propagation of oil impurities in seas and oceans and accidental emissions of hazardous substances at chemical plants. The propagation of gravity currents is frequently accompanied by disastrous damage; therefore, it is of interest to study the structure of such currents, the velocities of their propagation, and their dynamic effect on various obstacles.

The present paper gives results from an experimental study of the dynamic effect of an internal gravity current due to intrusion of a denser fluid into fresh water on a submerged circular cylinder. The structure of internal gravity currents of this type has been thoroughly studied both theoretically and experimentally. The main results of research on the problem in question are presented in [1]. In recent years, theoretical and numerical models of gravity currents taking into account the friction on the channel bottom and mixing effects have been actively developed [2, 3], and some experimental data have been obtained on the structure of the velocity field [4] and the density-field fluctuation spectrum at the current head [5]. Some papers have studied the interaction of gravity currents with various obstacles [6, 7]. However, the problem of determining the hydrodynamic loads resulting from the interaction of gravity currents with submerged bodies has not been considered previously. The objective of the present work was to study the characteristic times, magnitudes, and similarity criteria of the hydrodynamic loads and the flow pattern at different stages of interaction of the current with an obstacle and different positions of the obstacle relative to the bottom. The closest natural analog of this problem is turbidity currents in oceans, which are a great hazard to underwater cables and pipelines.

Experimental Technique. A diagram of the experimental setup is presented in Fig. 1. The experiments were performed in a $320 \times 20 \times 12$ cm hydrodynamic tank separated by partition 1 into two equal parts. The left half of the tank was filled with pure water of density ρ_1 and depth H , and the right half of the tank was filled with an aqueous solution of sugar of density ρ_2 and depth h_2 , above which there was a pure water layer of density ρ_1 and depth h_1 ; $h_1 + h_2 = H$. On the right half of the tank there was a streamlined body 2 (see Fig. 1), whose lower edge was at distance h_0 from the tank bottom and whose upper edge was at depth h_2 . In the experiments, the geometrical parameters had the following values: $H = 10$ cm, $h_2 = 8$ cm, and $h_0 = 2.3$ sec. When the partition

Lavrent'ev Institute of Hydrodynamics, Siberian Division, Russian Academy of Sciences, Novosibirsk 630090; ermanyuk@hydro.nsc.ru. Translated from *Prikladnaya Mekhanika i Tekhnicheskaya Fizika*, Vol. 46, No. 2, pp. 81–90, March–April, 2005. Original article submitted February 9, 2004; revision submitted July 7, 2004.

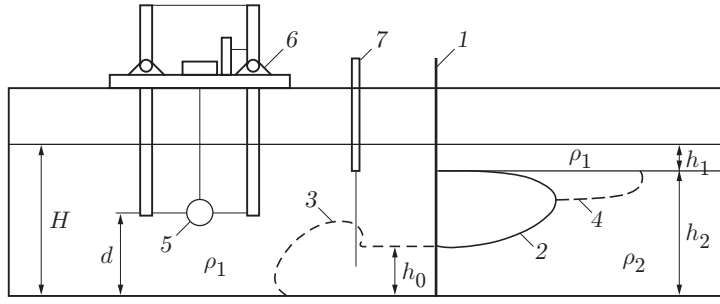


Fig. 1. Diagram of the experimental setup.

was removed, an internal gravity current 3 propagated to the left over the tank bottom, and a depression wave 4 propagated in the right part of the test tank (the dashed curves in Fig. 1). The propagation of a gravity current of the undular-bore type was also investigated. This flow pattern occurred in the case where under the pure-water layer in the left part of the tank there was a layer of an aqueous solution of sugar of density near the bottom ρ_2 . The density distribution parameters were measured using a technique similar to that used in [8]. In the experiments, the pycnocline thickness was $\delta = 0.6$ cm and the depth of the lower fluid layer was $h_3 = 0.6$ sec. The remaining parameters of the problem did not vary. In a coordinate system with origin at the tank bottom and the y axis directed vertically upward, the density distribution in the left part of the tank had the form

$$\rho(y) = \rho_0[1 - (\varepsilon/2) \tanh(2(y - h_3)/\delta)],$$

where $\rho_0 = (\rho_2 + \rho_1)/2$ and $\varepsilon = (\rho_2 - \rho_1)/\rho_1$.

The instantaneous hydrodynamic loads resulting from the interaction of gravity currents with a submerged circular cylinder 5 of diameter $D = 1.5$ cm were measured using a two-dimensional hydrodynamic balance 6 [8]. The center of the cylinder 5 was at $l = 4H$ from the partition 1 and at distance d from the tank bottom. The analog signals from the force sensors and wavemeter 7 were processed using a computer furnished with a 12-digit analog-to-digital converter. The gravity-current pattern and its interaction with the submerged cylinder were recorded with a digital camera. Visualization was performed using the following technique [9]: a luminous screen with a grid of inclined lines drawn on it was photographed through the water layer. In the zones with a high density gradient, the characteristic distortion of these lines was observed, and in the zones of active mixing there was a loss of the optical transparency of the fluid.

Experimental Results. It is known [4] that in the measurement zone, i.e., at $l = 4H$ from the partition, the gravity current is in a developed inertial regime (greater details of the main regimes of gravity currents at different stages of their development are discussed in [1]). In the inertial current regime, the velocity of the front V is nearly constant and is usually represented as the dependence of the Froude number $Fr = V/\sqrt{\varepsilon gh_*}$ (g is the acceleration of gravity and h_* is the thickness of the nonmixed core behind the current front) on the parameter $\alpha = h_*/H$. For a two-layer perfect fluid in the absence of mixing, the dependence $Fr(\alpha)$ was obtained for the first time in [10]. For a two-layer system of miscible viscous fluids, data on the dependence $Fr(\alpha)$ are given in [11], where it is also noted that according to visualization data, the gravity-current pattern ceases to depend on the Reynolds number $Re = Vh_*/\nu$ (ν is the kinematic viscosity of a fluid of density ρ_2) at $Re \approx 1000$.

The flow patterns in the absence of an obstacle at $\varepsilon = 0.02$ are given in Fig. 2 for the gravity current propagating over the channel bottom and for the undular bore propagating over a layer of density ρ_2 and depth $h_3 \neq 0$. In the case of the gravity current, the mixing zone encompasses the entire current head of depth about $2h_*$; behind the head, the thickness of the mixing zone is about $0.8h_*$. Measurements showed that for the thickness of the nonmixed core of the current, it is possible to set $h_* = h_0$. Under the experimental conditions, $Fr = 0.82$, which is in good agreement with the data of [1] for $\alpha = h_0/H = 0.23$.

During the propagation of the undular bore (Fig. 2b), a distinct mixing zone takes place only on the rear slope of the first undulation. For the undular bore under the conditions of the experiment, $Fr = 0.88$. Apparently, other conditions being equal, the higher propagation velocity of the undular bore with a smooth leading edge than that of the gravity current (Fig. 2a) is due to the smaller loss of the flow energy in mixing processes.

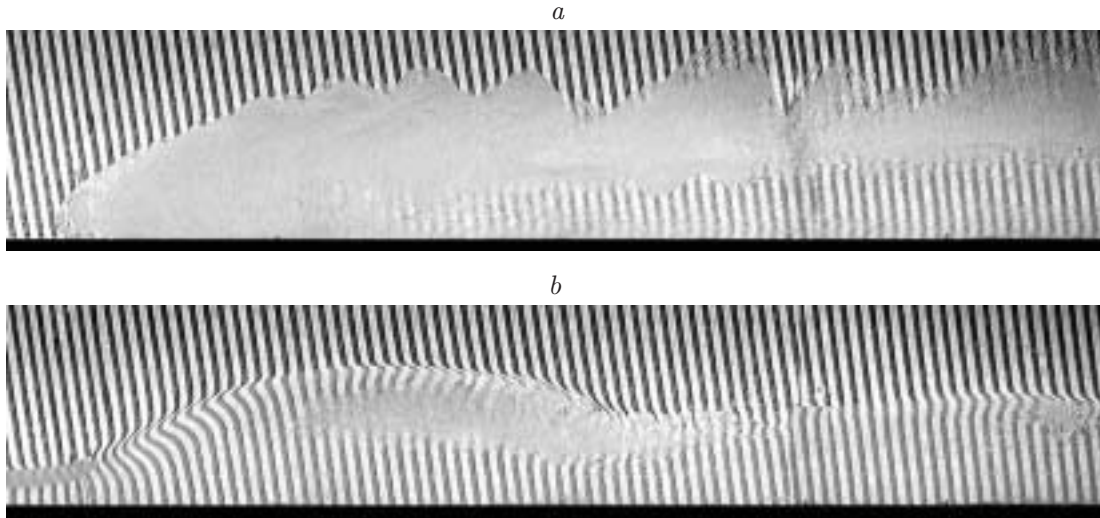


Fig. 2. Gravity current (a) and undular bore (b) structures.

Pictures of the interaction of the gravity current and the undular bore with the submerged circular cylinder are presented in Figs. 3 and 4, respectively. In terms of the dimensionless time with scale inversely proportional to $\sqrt{\varepsilon}$, the phases of flow development in these figures practically coincide.

As is evident from Fig. 3, the initial stage of interaction of the gravity current with the submerged cylinder involves the formation of a jet flow similar to that resulting from the impact of a body on a free surface. Next, in the stage of formation of the wave reflected from the submerged cylinder there is a considerable rise in the mixed-fluid level above the cylinder, and then, after a certain transient process of oscillatory nature, quasi-steady-state flow (Fig. 3e) is established, which is characterized by a considerable difference between the levels upstream and downstream of the obstacle. Flow of the hydraulic-jump type is formed downstream of the obstacle. The processes shown in Figs. 3 and 4 differ significantly in the degree of development of mixing effects. In addition, in the case of the undular bore, there is generation of downstream pulsations (Fig. 4c), which are the flow response to the interaction of the cylinder with the sequence of undulations.

In the stage of “impact” (intrusion of the body into the gravity-current front for a distance about D), one might expect hydrodynamic loads with a time scale $T_* = D/V$, and in the transitional oscillatory process of level change above the cylinder, hydrodynamic loads with a time scale $T = \sqrt{h_0/(\varepsilon g)}$. For the range of parameters studied in the present work, the shortest time scale is T_* (for the maximum value $\varepsilon = 0.04$, the time scale $T_* \approx 0.27$ sec). The hydrodynamic-balance design was such that the natural oscillation period for each of the degrees of freedom did not exceed 0.03 sec.

By analogy with the problem of body impact on water [11, 12], in the initial stage of interaction of the gravity current with the obstacle, we can assume that for hydrodynamic loads per unit length of cylinder $F_{x,y} \sim \rho V^2 D$. In the stage of quasi-steady-state flow there are a hydrostatic load component proportional to $\rho \varepsilon g D^2$ and a component proportional to the velocity head $\rho V_0^2 D^2/2$ (in the experiments, the average velocity in the nonmixed current core was $V_0 \cong 1.2V$ for the gravity current shown in Fig. 2a and $V_0 \cong 1.04V$ for the undular bore shown in Fig. 2b). Thus, for the unchanged initial geometrical parameters of the problem and a change in ε , the hydrodynamic loads should change by a factor of ε and the characteristic times by a factor of $\sqrt{\varepsilon}$; i.e., Froude simulation can be performed at all stages of the flow. Thus, it is assumed that the mixing processes, which determine the flow pattern at the gravity-current head, are simulated after Froude and the effect of the variation in the Reynolds number is insignificant.

The correctness of Froude simulation was investigated in the experiments performed for $d/D = 0.8$ and three values $\varepsilon = 0.01, 0.02$, and 0.04 . It should be noted that flow patterns were photographed in all experiments of this series. A comparison of photographs obtained for various ε taking into account the change in the time scale by a factor of $\sqrt{\varepsilon}$ shows complete similarity between the flows, including the fine details related to the development

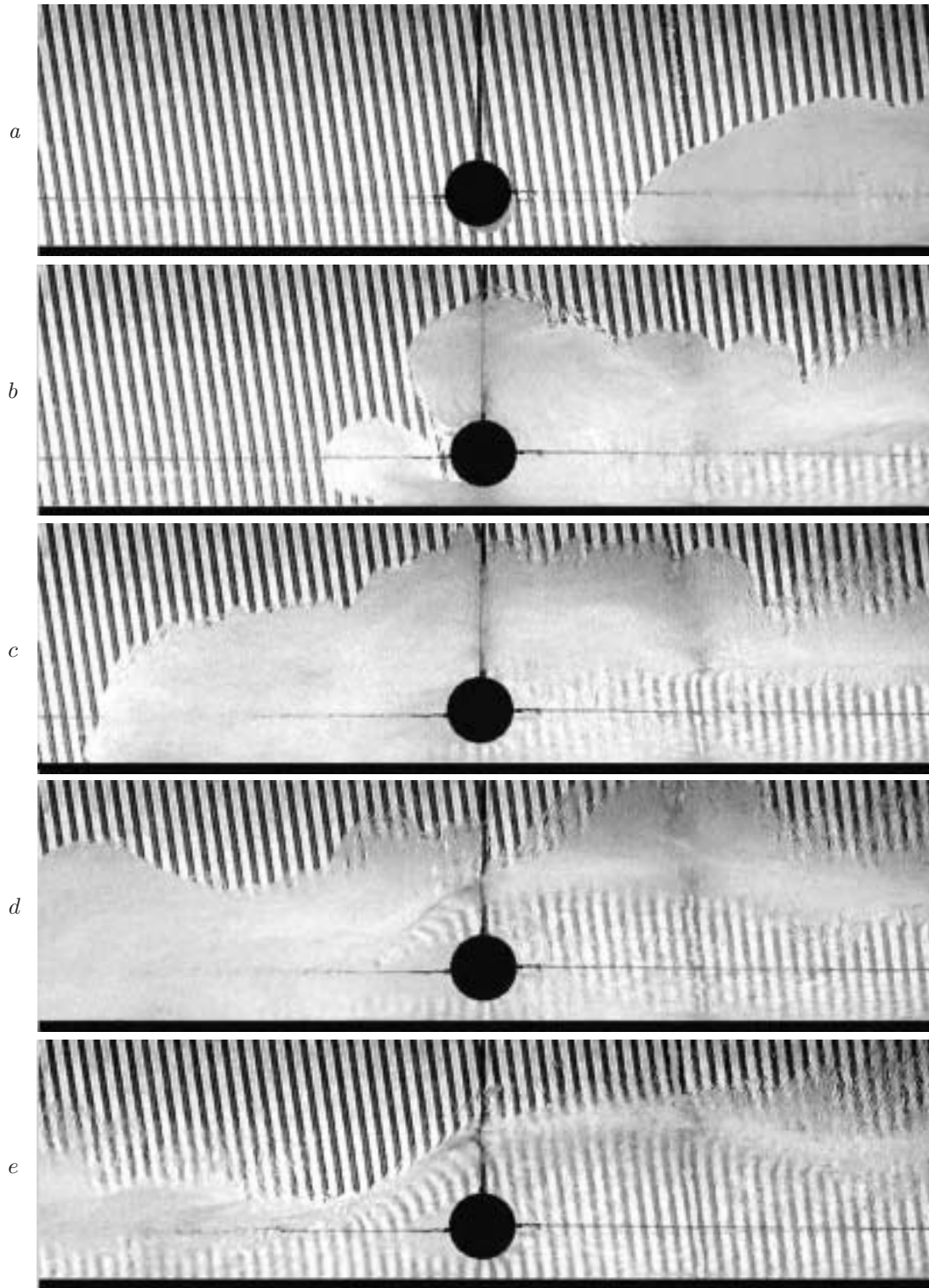


Fig. 3. Interaction of the gravity current with the submerged cylinder for $d/D = 0.8$ and $\varepsilon = 0.02$: the time step between frames a and d is $\Delta t = 1.33$ sec, and that between frames d and e is $\Delta t = 4.67$ sec.

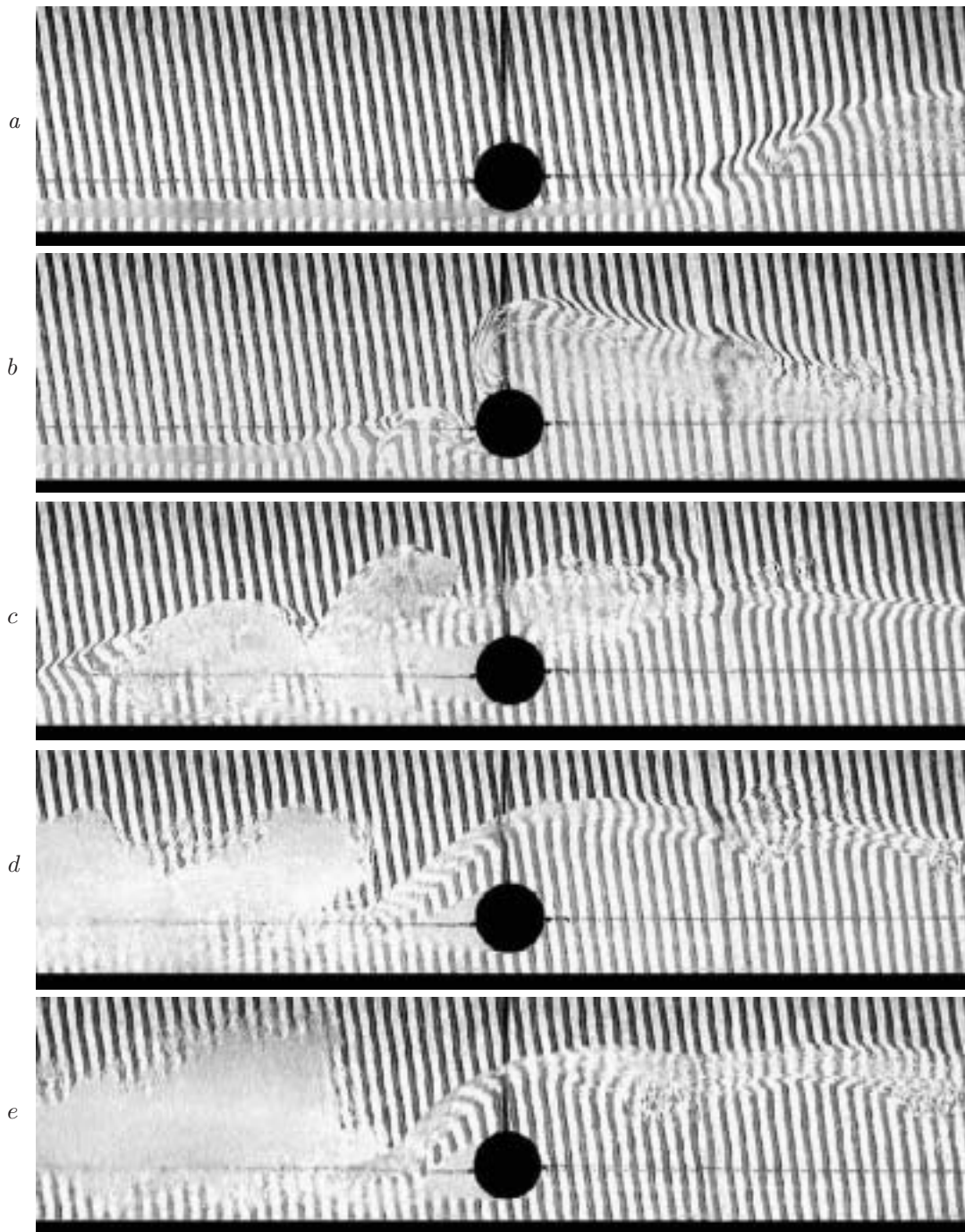


Fig. 4. Interaction of the undular bore with the submerged cylinder for $d/D = 0.8$ and $\varepsilon = 0.01$: the time step between frames a and d is $\Delta t = 2$ sec, and that between frames d and e is $\Delta t = 6.67$ sec.

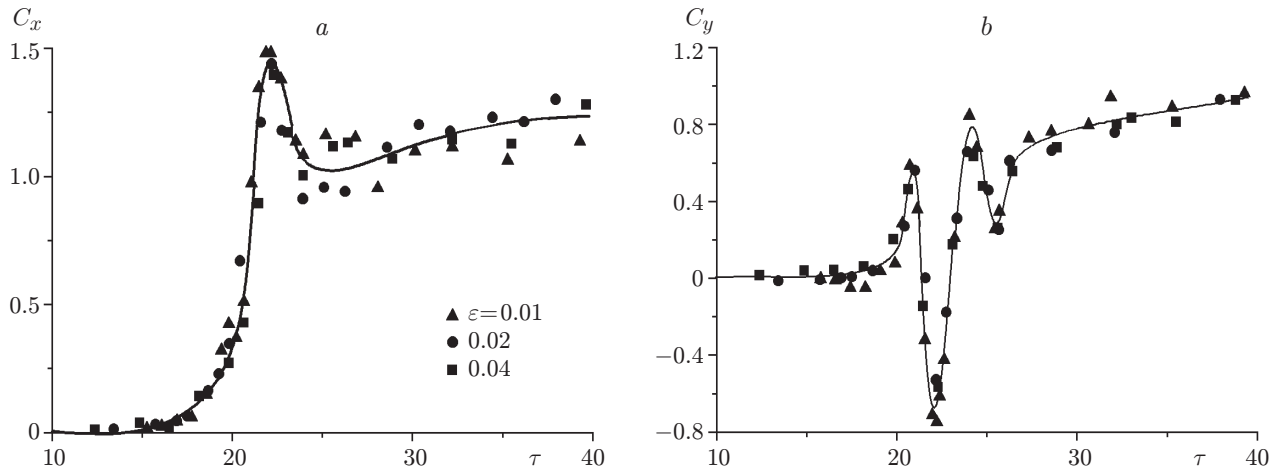


Fig. 5. Horizontal (a) and vertical (b) force coefficients versus dimensionless time for the incidence of the gravity current on the submerged cylinder for $d/D = 0.8$ and various values of ε .

of instability at the interface. The results of measurements of the loads due to the interaction of the gravity current with the obstacle (Fig. 3) obtained in this series of experiments are given in Fig. 5 for the horizontal and vertical force coefficients per unit length of the cylinder defined as $C_{x,y} = 4F_{x,y}/(\varepsilon\rho g\pi D^2)$. The dimensionless time $\tau = t\sqrt{\varepsilon g/h_0}$ is plotted on the abscissa. The time reference is the moment the front passes through the wavemeter 7 (see Fig. 1). As follows from Fig. 5, the dependences $C_x(\tau)$ and $C_y(\tau)$ obtained for different values of ε coincide with good accuracy. A similar result is obtained for the undular bore. This is further evidence for the substantially deterministic nature of the complex flow patterns shown in Figs. 3 and 4. The effect of random flow fluctuations on the hydrodynamic load is insignificant. We note that for ε varying in the range $0.01 \leq \varepsilon \leq 0.04$, the Reynolds number varies in the range $770 \leq \text{Re} \leq 900$ (the maximum value of Re is reached for $\varepsilon \approx 0.02$, and with further increase in ε , the Reynolds number decreases because of the rapid increase in the viscosity). In the experiments, the Schmidt number, which is defined as $\text{Sc} = \nu/\varkappa$ (\varkappa is the diffusion coefficient of the substance that produces stratification) was rather large and varied in the range $3400 \leq \text{Sc} \leq 6500$. Therefore, variation in the Schmidt number did not affect the results of the experiments. As a rule, the Schmidt number has a significant effect on the stability and integral characteristics of flow only if it varies over a wide range (by two orders of magnitude) [13].

The time dependences of the force coefficients $C_x(\tau)$ and $C_y(\tau)$ for various positions of the cylinder relative to the bottom d/D are given in Figs. 6 and 7 for the gravity current and undular bore shown in Fig. 2a and Fig. 2b, respectively. The results of this series of experiments were obtained for $\varepsilon = 0.02$. It should be noted that the maximum horizontal and vertical hydrodynamic loads are comparable, which indicates the importance of experimental and theoretical estimation of both force components. The hydrodynamic-load magnitudes are maximal when $d/D \approx 0.5$ (the cylinder lies on the bottom). In the stage of interaction with the current head, the dynamic loads are close to the quasi-steady-state loads developed at large times of interaction of the body with the gravity current. For $d/D \approx 0.5$, the vertical load is not alternating because of the suction force exerted on the cylinder by the current flowing over it.

The force coefficients can be defined in a similar manner as the standard coefficients of hydrodynamic resistance as $C_{x,y}^v = 2F_{x,y}/(\rho V^2 D)$. With this definition, $C_{x,y}^v = C_{x,y}\pi D/(2h_*\text{Fr}^2)$, which for the conditions of the experiments gives $C_{x,y}^v = 1.51C_{x,y}$ (gravity current) and $C_{x,y}^v = 1.32C_{x,y}$ (undular bore). For $d/D = 0.53$, the maximum values of the force coefficients $C_x^v \approx C_y^v \approx 2.3$ and $C_x^v \approx C_y^v \approx 1.8$ for the gravity current and undular bore, respectively. The marked difference between the values of the hydrodynamic coefficients (about 30 %) is due to an increase in the gradients of the flow parameters at the gravity-current front compared to the smooth head of the undular bore.

With increase in the value of d/D , the hydrodynamic loads decrease considerably, which is especially notable for the quasi-steady-state load acting at large times τ . Accordingly, the maximum dynamic effect of the flow on the submerged body occurs in the stage of interaction of the body with the current head. It should be noted that the vertical load is alternating in this case.

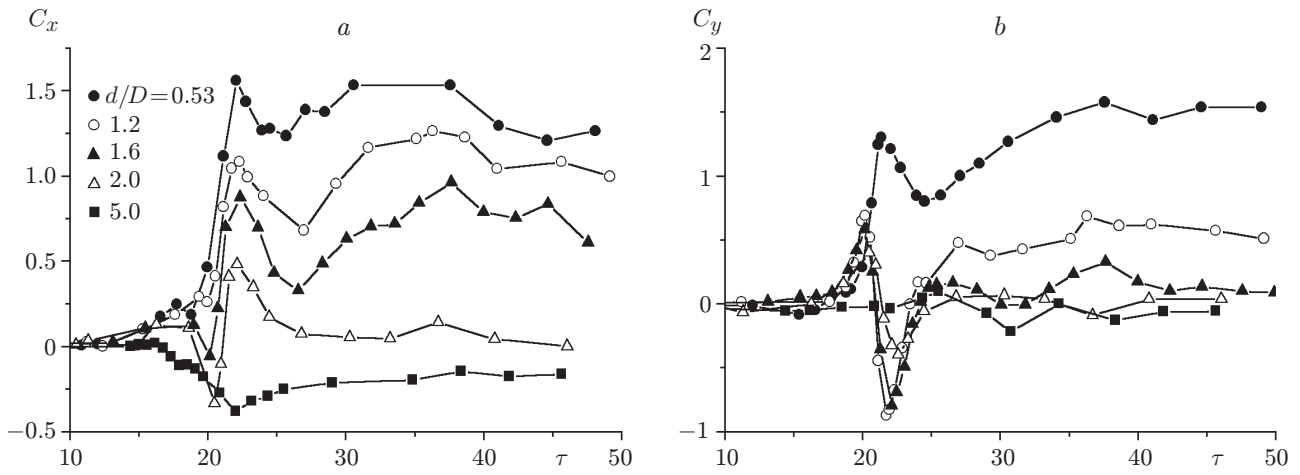


Fig. 6. Horizontal (a) and vertical (b) load coefficients versus dimensionless time for the incidence of the gravity current on the submerged cylinder for various d/D .

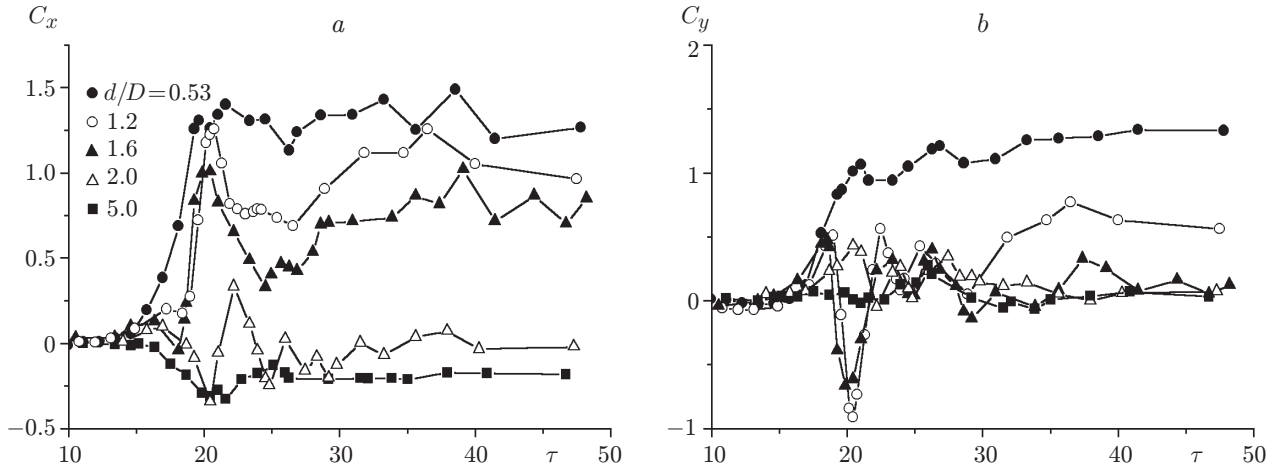


Fig. 7. Horizontal (a) and vertical (b) load coefficients versus dimensionless time for the incidence of the gravity current on the submerged cylinder for various d/D .

In applied problems, both the maximum values of hydrodynamic loads and the characteristic times of their pulsations are of significance. From Figs. 6 and 7 it follows that the characteristic time intervals between the neighboring maximum and minimum loads are $\Delta\tau \approx 5$ and $\Delta\tau \approx 2.5$. In these intervals of times, the current front has time to travel distances about $4h_0$ and $2h_0$, respectively. Apparently, these scales of lengths correspond to the main characteristic horizontal scales of the head structures of the currents considered.

An important difference in the nature of the hydrodynamic loads resulting from the interaction of the submerged body with the gravity current and undular bore is apparent from a comparison of the curves of the horizontal loads given in Fig. 6a and 7a. From physical considerations, it is obvious that for $d < h_0$ and $d \gg h_0$, one might expect that $C_x > 0$ and $C_x < 0$, respectively, because the denser and less dense fluids move in opposite directions. The value $d = h_0$ corresponds to $d/D = 1.4$. In a neighborhood of this value, one might expect positive or negative values of C_x , depending on the degree of mixing and distribution of the fluid velocity with depth. As a quantitative measure that characterizes the preferential effect of the upper or lower fluid layer on the cylinder in the time interval $\delta\tau = \tau_2 - \tau_1$, we introduce the quantity

$$K\left(\frac{d}{D}\right) = \frac{1}{\tau_2 - \tau_1} \int_{\tau_1}^{\tau_2} C_x\left(\frac{d}{D}, \tau\right) d\tau.$$

For the time interval from $\tau_1 = 10$ to $\tau_2 = 50$ shown in Figs. 6 and 7 and for $d/D = 0.53, 2,$ and 5 , the numerical values of K are equal to $1.16, 0.1,$ and -0.22 , respectively, for the gravity current, and $1.13, -0.03,$ and -0.21 , respectively, for the undular bore. For $d/D = 0.53$ and $d/D = 5$, the parameter K takes positive and negative values, respectively, and the numerical values of K are close in the two problems considered. For $d/D = 2$, the parameters K in the problems of the gravity current and undular bore differ both in value and sign. This is explained by the more developed mixing at the gravity-current front compared to the head of the undular bore and, hence, the more appreciable entrainment of the upper fluid layer in the motion of the lower layer. Since the hydrodynamic load is an integral characteristic of the momentum flux through control surface located upstream and downstream of the submerged cylinder, strong mixing and appreciable entrainment indicate that in the theoretical description of the problem, it is necessary to use mathematical models of type [2] that take into account mixing and entrainment effects and the real velocity distributions with depth.

Conclusions. The present study of the structures of a gravity current with a mixed leading edge and a current of the undular-bore type and their dynamic effects on a submerged circular cylinder showed that the hydrodynamic loads are maximal if the cylinder lies on the channel bottom and the horizontal- and vertical-load magnitudes are comparable. The gravity current with a mixed leading edge exerts a greater dynamic effect on the submerged body than the undular bore propagating under similar conditions. Under the conditions of the experiments performed, the hydrodynamic loads are simulated after Froude.

This work was supported by integration project No. 3.13.1 of the Siberian Division of the Russian Academy of Sciences and interdisciplinary project No. 131 the Siberian Division of the Russian Academy of Sciences.

REFERENCES

1. J. E. Simpson, *Gravity Currents: In the Environment and Laboratory*, Cambridge Univ. Press, Cambridge (1997).
2. V. Yu. Liapidevskii and V. M. Teshukov, "Mathematical models for the propagation of long waves in an inhomogeneous fluid," *Izd. Sib. Otd. Ross. Akad. Nauk*, Novosibirsk (2000).
3. C. Hartel, E. Meiburg, and F. Meiburg, "Analysis and direct numerical simulation of the flow at a gravity-current head. 1. Flow topology and front velocity for slip and no-slip boundary," *J. Fluid Mech.*, **41**, 189–212 (2000).
4. L. P. Thomas, S. B. Dalziel, and B. M. Marino, "The structure of the head of an inertial gravity current determined by particle-tracking velocimetry," *Exper. Fluids*, **34**, 708–716 (2003).
5. J. D. Parsons and M. H. Garcia, "Similarity of gravity flow fronts," *Phys. Fluids*, **10**, No. 12, 3209–3213 (1998).
6. J. W. Rottman, J. E. Simpson, J. S. R. Hunt, and R. E. Britter, "Unsteady gravity flows over obstacles," *J. Hazardous Mat.*, **11**, 325–340 (1985).
7. G. F. Lane-Serff, L. M. Beal, and T. D. Hadfield, "Gravity flow over obstacles," *J. Fluid Mech.*, **292**, 39–53 (1995).
8. N. V. Gavrilov and E. V. Ermanyuk, "Effect of a pycnocline on forces exerted by internal waves on a stationary cylinder," *J. Appl. Mech. Tech. Fiz.*, **37**, No. 6, 825–831 (1996).
9. V. I. Bukreev and N. V. Gavrilov, "Perturbations ahead of a wing moving in a stratified fluid," *J. Appl. Mech. Tech. Fiz.*, No. 2, 257–259 (1990).
10. T. B. Benjamin, "Gravity flows and related phenomena," *J. Fluid Mech.*, **31**, pt 2, 209–248 (1968).
11. M. Moghisi and P. T. Squire, "An experimental investigation of the initial force of impact on a sphere striking a fluid surface," *J. Fluid Mech.*, **108**, 133–146 (1981).
12. L. I. Sedov, *Similarity and Dimension Methods in Mechanics* [in Russian], Nauka, Moscow (1972).
13. V. I. Bukreev, A. V. Gusev, and E. M. Romanov, "Effect of molecular diffusion on the stability of stratified shear flows," *Izv. Ross. Akad. Nauk, Mekh. Zhidk. Gaza*, No. 1, 35–40 (1993).